‘Sweeping rods’: cargo transport by self-propelled bimetallic microrods moving perpendicular to their long axis

Peer-reviewed author version

Arslanova, Alina; Dugyala, Venkateshwar Rao; Reichel, Erwin Konrad; REDDY, Naveen; Fransaer, Jan & Clasen, Christian (2021) ‘Sweeping rods’: cargo transport by self-propelled bimetallic microrods moving perpendicular to their long axis. In: Soft Matter, 17 (9), p. 2369 -2373.

DOI: 10.1039/d1sm00042j
Handle: http://hdl.handle.net/1942/34196

Journal Name

ARTICLE TYPE

Cite this: DOI: 00.0000/xxxxxxxxxx

‘Sweeping rods’: Cargo transport by self-propelled bimetallic microrods moving perpendicular to their long axis†

Alina Arslanova,[a] Venkateshwar Rao Dugyala [b], Erwin Konrad Reichel [c], Naveen Reddy,[d,e] Jan Fransaer,[f] and Christian Clasen *[a]

Received Date
Accepted Date

DOI: 00.0000/xxxxxxxxxx

A possible application of self-propelling particles is the transport of microscopic cargo. Maximizing the collection and transport efficiency of particulate matter requires the area swept by the moving particle to be as large as possible. One such particle geometry are rods propelled perpendicular to their long axis, that act as "sweepers" for collecting particles. Here we report on the required Janus coating to achieve such motion, and on the dynamics of the collection and transport of microscopic cargo by sideways propelled Janus rods.

Cargo manipulation at micro- and nano-scales is a challenging, yet desirable task for targeted drug delivery[1,2], microrobotics[3,4], operating and separating particles and biological matter at the microscale[5–9], as well as removing unwanted species from a solution[2,10]. Pick-up, delivery and drop-off of the cargo can be performed by autonomously moving micro- and nano-motors[11,12]. There were many successfull attemps of exploiting biological motors, such as bacteria, for that task[13–16]. However, artificial active particles still remain beneficial for a range of applications in particular due to the tunability of their properties, as well as a more precise motion control[17–19]. Among active particles, Janus particles play a crucial role in manipulating the matter at the microscale. Janus particles have two distinct surfaces different in chemical or physical properties, allowing them to create a gradient of a physical parameter in their proximity that generates a fluid flow along the particle, inducing particle motion[20–22]. When Janus particles are mixed with passive tracers, they show different interactions depending on the type of the active coating and are able to collect and transport cargo when interactions are attractive[23]. To ensure transport of a specific cargo, most of the studied systems exploit specific interactions between the cargo and the Janus particle, as for example electrostatic interaction between polypyrrole segment and charged cargo[24], interactions with biological molecule moieties[24–26], magnetic[27,28] or hydrophobic interactions[10,29,30]. Moreover, cargo transport was shown also for Janus particles with no surface functionalization but possessing a permanent magnetic moment[31].

While the above approaches are applicable for the pick-up of specific types of cargo, the manipulation of general non-specific loads is also of interest, for instance for the ‘sweeping’ of unwanted or dangerous species in a solution. However, studies of assemblies of non-functionalized active and passive particles are still limited. The transport of non-functionalized cargo was shown for micro-tubular motors propelled at air-water inteface[32] and in microfluidic channel[33]. Label-free pick-up of cargo was also carried out by dielectrophoresis for spherical Janus particles[34–36] and by electrokinetic mechanism for Janus nano-rods propelling along their long axis[37]. However, for the efficient pick-up of cargo it is preferable to produce Janus particles with larger active surface area, as, for example, rods propelled perpendicular to their long axis. Such sideways propelled rods were recently fabricated and their general movement was studied[38–40], but the possibility and dynamics of cargo transport by this system has not been investigated yet, which is the subject of this communication. The fabrication of Janus rods was adapted from previous publications[38,39]. A monolayer of aligned 3 μm diameter polystyrene fibers was produced by electrospinning a 25 wt.% solution of

[a] *Department of Chemical Engineering, KU Leuven, 3001 Leuven, Belgium*
[b] *Department of Chemical Engineering, Indian Institute of Science Education and Research Bhopal, Bhopal Bypass Road, Bhauri, Bhopal 462 066, Madhya Pradesh, India*
[c] *Institute for Microelectronics and Microsensors, Johannes Kepler University, Altenberger Strasse 69, 4040 Linz, Austria*
[d] *Faculty of Engineering Technology, University of Hasselt, Martelarenlaan 42, 3500 Hasselt, Belgium*
[e] *IMO-IMOMEC, Wetenschapspark 1, 3590 Diepenbeek, Belgium*
[f] *Department of Materials Engineering, KU Leuven, 3001 Leuven, Belgium*
* Author to whom any correspondence should be addressed. *Fax: +32 16 3 22 991; Tel: +32 16 32 23 54; E-mail: christian.clasen@kuleuven.be*
† Electronic Supplementary Information (ESI) available: [details of any supplementary information available should be included here]. See DOI: 00.0000/00000000.

polystyrene (PS, $M_w = 280$ kg mol^{-1}, Sigma Aldrich BVBA) in N,N-dimethylformamide (DMF, 99.8 %, Acros Organics NV); parameters of electrospinning: voltage - 22 kV, flow rate - 0.2 ml h^{-1}, needle diameter - 0.61 mm, temperature - 34 °C, relative humidity - 25 RH, distance between the needle and collector - 13.5 cm. The alignment of fibers was achieved by using rectangular parallel electrodes[39,41] or a rotating drum collector (speed $1000-2000$ rpm) coupled with translating unit[42] (MTI, MSK-ESDC-3000). In the first approach, fibers are aligned parallel when randomly jumping from one parallel electrode plate to the other, while for the second approach fibers are aligned via the additional elongation force exerted by the rotating drum on the fibers[43]. The obtained fiber monolayer was subsequently sputter coated (Quorum, Q150TS) with 5 nm thick Pt and Au layers on opposing sides of the layer respectively, resulting in long Janus fibers. After dispersing the Janus fibers in water, they were cut into smaller rods of $10-100$ μm length by ultrasonication using an ultrasonic probe (Hielscher UP400S, power density 450 W cm^{-2}) for 1.5 min. This produces rods with a broad length distribution, as well as bent rods.

The sideways self-propulsion of Pt/Au rods in hydrogen peroxide (2.8 wt.%, pH = 4.5) containing polystyrene sulfate spheres (Invitrogen^{TM}, diameter $d = 3$ μm, 8 w/v%) as the cargo, is captured with an inverted optical microscope (Olympus, IX71) at different magnifications (50x, 20x). All self-propulsion experiments were carried out in a glass cell with a 1.5 mm deep, round well (diameter $d = 13$ mm). When the rods are placed in the hydrogen peroxide solution, they settle and propel near the bottom wall due to their slightly higher density and size.

Different driving forces for the propulsion of bimetallic Janus rods were proposed in literature, such as self-induced electric fields, concentration gradients, or surface tension gradients[44,45]. Although the exact mechanism of their motion is not understood yet, a strong evidence was obtained for a dominating self-electrophoretic propulsion mechanism, and it was shown that such bimetallic rods are moving with their platininum segment facing forward[46,47]. The close proximity of the particles to the wall further influences their motion due to electroosmotic flow[48,49]. Since a small fraction of rods got intermediately stuck on the surface, we selected for the analysis rods of length ~ 20 μm that exhibited a stable motion within the experimental observation time (~ 5 min). The images were analyzed using a self-written Python code‡ to determine the particles trajectories and velocities as a function of cargo loading.

When dispersed in hydrogen peroxide solution containing polystyrene spheres with sulfate surface groups, the Janus rods 'sweep' the solution near the bottom wall, capturing cargo particles as shown in Fig. 1. The self-propulsion experiments in Fig. 1 (additionally, see movie M1 in the supporting information) are carried out in a dilute dispersion of cargo spheres, to ensure that the sideways self-propelling rod captures the cargo spheres, that undergo Brownian motion by themselves, one at a time.

‡ The Python code for the tracking of the rods motion: `https://github.com/ReknowIndra/rod-track`

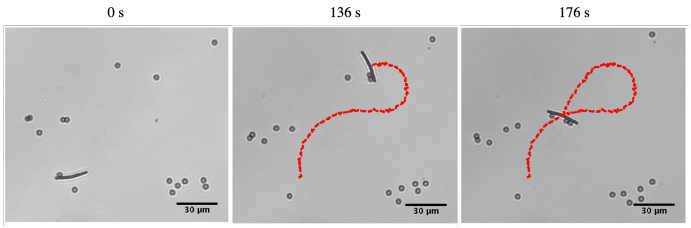

Fig. 1 Sideways propelled Pt/Au rod collecting polystyrene cargo particles (~ 0.005w/v%) in aqueous hydrogen peroxide (2.8 wt.%), scale bar is 30 μm.

The rod velocity decreases with increasing number of captured spheres due to an increase in the resistance of the microrod-cargo aggregate to the flow (Fig. 2), in agreement with studies on the drag resistance of the rafts of spherical objects[12,32]. A simple formula for the velocity of a microswimmer-cargo aggregate was derived by Raz and Leshansky[50]:

$$V_{\mathrm{d}} = \frac{V_{\mathrm{r}} K_{\mathrm{r}}}{K_{\mathrm{r}} + K_{\mathrm{l}}}, \tag{1}$$

where V_{d} is the velocity of the microswimmer dragging the spheres $\left[\mathrm{m\ s^{-1}}\right]$, V_{r} and K_{r} are the velocity $\left[\mathrm{m\ s^{-1}}\right]$ and the resistance coefficient $\left[\mathrm{kg\ s^{-1}}\right]$ of the swimmer without cargo, respectively, and K_{l} is the resistance coefficient of the cargo $\left[\mathrm{kg\ s^{-1}}\right]$.

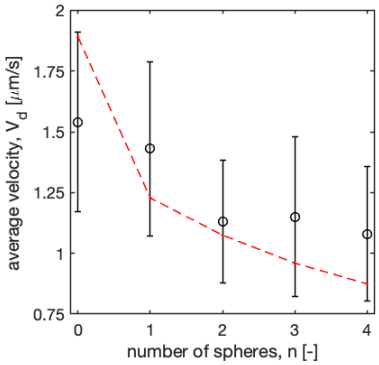

Fig. 2 Velocities of a sideways propelled Janus rods of length ~ 20 μm that are pushing n polystyrene spheres in aqueous hydrogen peroxide (2.8 wt.%) solution (averaged for each loading over 3 different rods). The dashed red line represents the velocities calculated from eq. 1 with a resistance coefficient of the rod K_{r} calculated from eq. 2, and the resistance coefficient of n polystyrene spheres K_{l} obtained from the beads model.

The resistance coefficient of a cylinder of radius r near a wall is given by[51]:

$$K_{\mathrm{r}} = \frac{4\pi}{\log\left[r^{-1}\left(d + |d^2 - r^2|^{0.5}\right)\right]}, \tag{2}$$

where d is the distance between the rod and the wall [m], which is determined by the balance of the gravitational force $F_{g,\mathrm{r}}$ and the electrostatic repulsion of the wall $F_{e,\mathrm{r}}$ per unit length[52,53]:

$$F_{e,\mathrm{r}} = 2\sqrt{2\pi}\varepsilon_0\varepsilon\kappa\sqrt{\kappa r}\times$$

$$\times\left[\zeta_w\zeta_r\exp(-\kappa h) - \frac{1}{\sqrt{2}}\left(\zeta_w^2+\zeta_r^2\sqrt{\frac{r}{r+h}}\right)\exp(-2\kappa h)\right], \quad (3)$$

$$\kappa = \sqrt{\frac{2\mathrm{F}^2 C_0}{\varepsilon_0\varepsilon \mathrm{R}T}}, \quad (4)$$

$$F_{g,\mathrm{r}} = -\pi r^2\Delta\rho g, \quad (5)$$

where $\varepsilon_0 = 8.85\cdot10^{-12}$ $\left[\mathrm{F\ m^{-1}}\right]$ is the vacuum permittivity, $\varepsilon = 80$ is the relative permittivity of water $[-]$, F is the Faraday constant $\left[\mathrm{C\ mol^{-1}}\right]$, $\kappa^{-1}\approx10^{-6}$ [m] is the Debye length calculated from eq. 4 with $C_0 = 0.0316$ $\left[\mathrm{mol\ m^{-3}}\right]$ as the bulk concentration of protons calculated from $\mathrm{pH} = -\log C_0$ at a pH $= 4.5$, $r = 1.5\ \cdot10^{-6}$ [m] is the rod radius, ζ_w is the zeta potential of the glass wall [V], ζ_r is the zeta potential of the rod [V], g is the gravitational acceleration $\left[\mathrm{m\ s^{-2}}\right]$, and $\Delta\rho = 50$ $\left[\mathrm{kg\ m^{-3}}\right]$ is the density difference between water and polystyrene. From balancing the electrostatic repulsion and gravitational acceleration, $F_{e,\mathrm{r}} = -F_{g,\mathrm{r}}$, and by assuming literature values for the zeta-potential of the rod and the wall of $\zeta_r = \frac{\zeta_{\mathrm{Pt}}+\zeta_{\mathrm{Au}}}{2}\approx-50\,\mathrm{mV}$ [17,37,54] and $\zeta_w\approx-40\,\mathrm{mV}$ [55], respectively, the separation distance between the rod and the bottom wall (d) is approximately 550 nm.

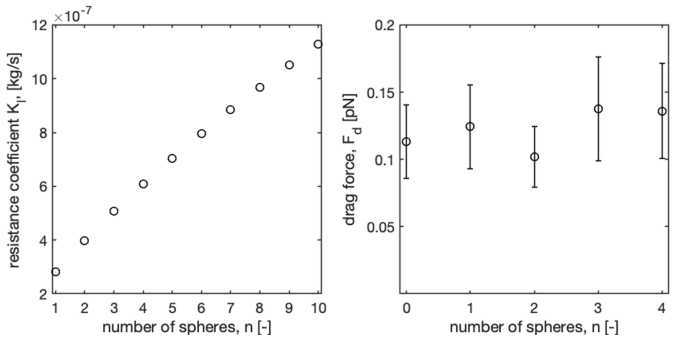

Fig. 3 On the left: resistance coefficient K_l as a function of the number of spheres n attached to the sideways moving rod. On the right: drag force on a sideways propelled rod with n-attached spheres in aqueous hydrogen peroxide (2.8 wt.%) solution.

To our knowledge, there is no analytical expression for the resistance coefficient of aggregates of several spheres K_l near the wall required in eq. 1. That resistance coefficient K_l can be found from the grand resistance matrix $\mathscr{H}$ defined as follows:

$$\begin{pmatrix} U_x \\ U_y \\ \dot{\phi} \end{pmatrix} = \mathscr{H}^{-1}\begin{pmatrix} F_x \\ F_y \\ T \end{pmatrix}, \quad (6)$$

where U_x and U_y are the microrod-cargo aggregate velocity in the direction perpendicular (x-direction) and parallel (y-direction) to the long axis of the solo-rod $\left[\mathrm{m\ s^{-1}}\right]$, $\dot{\phi}$ is the aggregate angular velocity $\left[\mathrm{s^{-1}}\right]$, $\mathscr{H}^{-1}$ is the mobility matrix of the microrod-cargo aggregate, F_x and F_y are the drag forces in the x and y direction [N], and T is the torque on the aggregate acting at the centre of mass [N m]. Therefore, the grand resistance matrix $\mathscr{H}$ for n touching beads is calculated using a beads model following the procedure detailed in [39], which takes into account the hydrodynamic interaction between the spherical particles but neglects initially any wall effects [56,57]. The relation between the resistance coefficient of the aggregate K_l and the number of spheres, n, is visualized in Fig. 3.

The resulting scaling of the velocity with the number of polystyrene spheres from eq. 1 is shown in Fig. 2. As the velocity of only the rod V_r is obtained within an error of 20%, it was adjusted by fitting the experimental data with eq. 1. The obtained scaling is in good agreement with the experimental values, albeit not a proof of the functional form, even though the wall effects for the aggregate of spheres is not accounted for in this model.

Aggregates of Janus sideways propelled rods and cargo particles are in general stable over the experimental time range, only for few cases it was observed that single sphere detached after a short time (~ 5 s), which we attribute to the slight differences in the sphere-wall distance for different spheres caused by their variation of density and consequently a misalignment of the rod and the sphere in z-direction.

According to Wang *et al.* [37], the cargo spheres are not only hydrodynamically dragged by the rod, but an additional attachment of the spheres to the rod is caused by the self-induced electric field arising from a self-electrophoretic mechanism. According to this, the negatively charged particles move up to the electric field, towards the platinum side of the Janus particle, which acts as an anode. Note that, unlike for rods propelled along their long axis [12], polystyrene spheres could attach also to the top side of the sideways propelled rods, although this configuration is highly unstable in the presence of the hydrodynamic drag.

Finally, the drag force on the aggregate was calculated using the approach developed by Hagen *et al.* [58–60]. The self-propelling force, which equals the drag force, obeys the relation for an identical passive particle under an external force and torque (eq. 6). The grand resistance matrix $\mathscr{H}$ was determined using again the beads model, now for the full aggregate. The drag force on the aggregate is then found by iteratively fitting eq. 6 to experimentally observed velocity of the microrod-cargo aggregate. Fig. 3 shows that the drag force on the microswimmer-cargo aggregate remains independent of the number of spheres, indicating that the attachment of spheres does not affect the propulsion force of the rod, and that the decrease in velocity in Fig. 2 is related solely to the increase of the hydrodynamic drag of the microswimmer-cargo aggregate.

The observed maximum loading indicates that the spheres themselves do not stick, but, as expected, due to their slight repulsive potential stack in the hydrodynamically most favored configuration on the first row of particles (that interacts with the rod as discussed above): a triangular closed packed state as observed in Fig. 4.

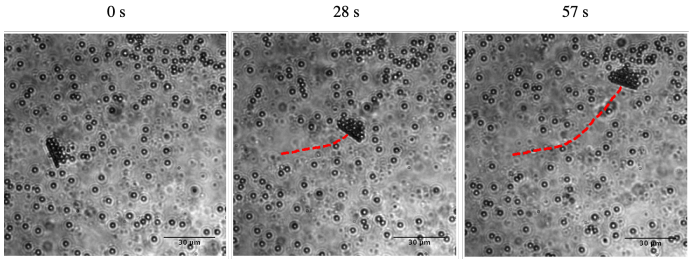

Fig. 4 Sideways propelled Pt/Au rod collecting polystyrene cargo particles (~ 0.02w/v%) in aqueous hydrogen peroxide (2.8 wt.%), scale bar is 30 μm.

In conclusion, we studied the collection and transport of microscale cargo by sideways propelled Janus rods, which are of interest due to their larger surface area for collecting cargo. Therefore, these rods can be used for "sweeping" the solution near the wall from unwanted or dangerous particles. The propulsion force on the rod remains unaffected by attached particles, but the velocity of microswimmer-cargo aggregate depends on the number of spheres it transports. Since the drag force remains constant, this velocity decrease is related to the increase in resistance coefficients of microswimmer-cargo aggregate through the addition of extra spheres. We connected the velocity decrease to the number of attached spheres via a simple model that takes the resistance coefficients of the several sphere aggregates into account via a beads model.

Conflicts of interest

There are no conflicts to declare.

Acknowledgements

The authors would like to acknowledge financial support from the FWO (Research Foundation Flanders, FWO project G077916N). E.K.R. acknowledges the Austrian Science Fund (FWF)/Research Foundation Flanders (FWO) project ZeoDirect I 3680-N34 and the LCM – K2 Center for Symbiotic Mechatronics (Austrian COMET-K2 program) for funding.

Notes and references

1 L. Sonntag, J. Simmchen and V. Magdanz, *Molecules*, 2019, **24**, 3410.
2 D. Patra, S. Sengupta, W. Duan, H. Zhang, R. Pavlick and A. Sen, *Nanoscale*, 2013, **5**, 1273–1283.
3 Y. Alapan, B. Yigit, O. Beker, A. F. Demirörs and M. Sitti, *Nature Materials*, 2019, 1.
4 H. Ceylan, J. Giltinan, K. Kozielski and M. Sitti, *Lab on a Chip*, 2017, **17**, 1705–1724.
5 C. Maggi, J. Simmchen, F. Saglimbeni, J. Katuri, M. Dipalo, F. De Angelis, S. Sanchez and R. Di Leonardo, *Small*, 2016, **12**, 446–451.
6 S. Balasubramanian, D. Kagan, C.-M. Jack Hu, S. Campuzano, M. J. Lobo-Castañon, N. Lim, D. Y. Kang, M. Zimmerman, L. Zhang and J. Wang, *Angewandte Chemie International Edition*, 2011, **50**, 4161–4164.
7 S. Sanchez, A. A. Solovev, S. Schulze and O. G. Schmidt, *Chemical Communications*, 2011, **47**, 698–700.
8 S. Campuzano, J. Orozco, D. Kagan, M. Guix, W. Gao, S. Sattayasamitsathit, J. C. Claussen, A. Merkoçi and J. Wang, *Nano letters*, 2012, **12**, 396–401.
9 J. Orozco, S. Campuzano, D. Kagan, M. Zhou, W. Gao and J. Wang, *Analytical chemistry*, 2011, **83**, 7962–7969.
10 M. Guix, J. Orozco, M. García, W. Gao, S. Sattayasamitsathit, A. Merkoçi, A. Escarpa and J. Wang, *Acs Nano*, 2012, **6**, 4445–4451.
11 L. Zhang, T. Petit, Y. Lu, B. E. Kratochvil, K. E. Peyer, R. Pei, J. Lou and B. J. Nelson, *ACS nano*, 2010, **4**, 6228–6234.
12 J. Wang, *Lab on a chip*, 2012, **12**, 1944–1950.
13 D. B. Weibel, P. Garstecki, D. Ryan, W. R. DiLuzio, M. Mayer, J. E. Seto and G. M. Whitesides, *Proceedings of the National Academy of Sciences*, 2005, **102**, 11963–11967.
14 L. Vaccari, M. Molaei, R. L. Leheny and K. J. Stebe, *Soft matter*, 2018, **14**, 5643–5653.
15 R. R. Trivedi, R. Maeda, N. L. Abbott, S. E. Spagnolie and D. B. Weibel, *Soft Matter*, 2015, **11**, 8404–8408.
16 N. Dogra, H. Izadi and T. K. Vanderlick, *Scientific reports*, 2016, **6**, 29369.
17 S. Das, A. Garg, A. I. Campbell, J. Howse, A. Sen, D. Velegol, R. Golestanian and S. J. Ebbens, *Nature communications*, 2015, **6**, 1–10.
18 L. Baraban, D. Makarov, O. G. Schmidt, G. Cuniberti, P. Leiderer and A. Erbe, *Nanoscale*, 2013, **5**, 1332–1336.
19 W. Z. Teo and M. Pumera, *Chemistry–A European Journal*, 2016, **22**, 14796–14804.
20 S. Ebbens and J. Howse, *Soft Matter*, 2010, **6**, 726–738.
21 W. Wang, W. Duan, S. Ahmed, T. E. Mallouk and A. Sen, *Nano Today*, 2013, **8**, 531–554.
22 A. Walther and A. H. Müller, *Soft Matter*, 2008, **4**, 663–668.
23 P. Chattopadhyay and J. Simmchen, 2019.
24 S. Sundararajan, P. Lammert, A. Zudans, V. Crespi and A. Sen, *Nano Lett*, 2008, **8**, 1271–1276.
25 J. Simmchen, A. Baeza, D. Ruiz, M. J. Esplandiu and M. Vallet-Regí, *Small*, 2012, **8**, 2053–2059.
26 S. Sundararajan, S. Sengupta, M. E. Ibele and A. Sen, *Small*, 2010, **6**, 1479–1482.
27 J. Burdick, R. Laocharoensuk, P. M. Wheat, J. D. Posner and J. Wang, *Journal of the American Chemical Society*, 2008, **130**, 8164–8165.
28 D. Kagan, R. Laocharoensuk, M. Zimmerman, C. Clawson, S. Balasubramanian, D. Kang, D. Bishop, S. Sattayasamitsathit, L. Zhang and J. Wang, *Small*, 2010, **6**, 2741–2747.
29 W. Gao, A. Pei, X. Feng, C. Hennessy and J. Wang, *Journal of the American Chemical Society*, 2013, **135**, 998–1001.
30 L. Baraban, M. Tasinkevych, M. Popescu, S. Sanchez, S. Dietrich and O. Schmidt, *Soft Matter*, 2012, **8**, 48–52.
31 G. Zhao, H. Wang, S. Sanchez, O. G. Schmidt and M. Pumera, *Chemical Communications*, 2013, **49**, 5147–5149.
32 A. A. Solovev, S. Sanchez, M. Pumera, Y. F. Mei and O. G. Schmidt, *Advanced Functional Materials*, 2010, **20**, 2430–2435.
33 S. Sanchez, A. A. Solovev, S. M. Harazim and O. G. Schmidt, *Journal of the American Chemical Society*, 2011, **133**, 701–703.
34 A. M. Boymelgreen, T. Balli, T. Miloh and G. Yossifon, *Nature communications*, 2018, **9**, 1–8.
35 Y. Wu, A. Fu and G. Yossifon, *Science Advances*, 2020, **6**, eaay4412.
36 A. F. Demirörs, M. T. Akan, E. Poloni and A. R. Studart, *Soft Matter*, 2018, **14**, 4741–4749.
37 W. Wang, W. Duan, A. Sen and T. E. Mallouk, *Proceedings of the National Academy of Sciences*, 2013, **110**, 17744–17749.
38 N. Reddy, L. Palangetic, L. Stappers, J. Buitenhuis, J. Fransaer and C. Clasen, *J. Mater. Chem.*, 2013, **1**, 3646.
39 V. R. Dugyala, N. Reddy, J. Fransaer and C. Clasen, *Journal of Physics D: Applied Physics*, 2018, **52**, 014002.
40 H. R. Vutukuri, Z. Preisler, T. H. Besseling, A. Van Blaaderen, M. Dijkstra and W. T. Huck, *Soft Matter*, 2016, **12**, 9657–9665.
41 D. Li, Y. Wang and Y. Xia, *Nano letters*, 2003, **3**, 1167–1171.
42 B. Sundaray, V. Subramanian, T. Natarajan, R.-Z. Xiang, C.-C. Chang and W.-S. Fann, *Applied physics letters*, 2004, **84**, 1222–1224.
43 M. Afshari, *Electrospun nanofibers*, Woodhead Publishing, 2016.
44 W. F. Paxton, K. C. Kistler, C. C. Olmeda, A. Sen, S. K. St. Angelo, Y. Cao, T. E. Mallouk, P. E. Lammert and V. H. Crespi, *Journal of the American Chemical Society*, 2004, **126**, 13424–13431.
45 W. F. Paxton, A. Sen and T. E. Mallouk, *Chemistry–A European Journal*, 2005, **11**, 6462–6470.
46 W. F. Paxton, P. T. Baker, T. R. Kline, Y. Wang, T. E. Mallouk and A. Sen, *Journal of the American Chemical Society*, 2006, **128**, 14881–14888.
47 Y. Wang, R. M. Hernandez, D. J. Bartlett, J. M. Bingham, T. R. Kline, A. Sen and T. E. Mallouk, *Langmuir*, 2006, **22**, 10451–10456.
48 W. Wang, T.-Y. Chiang, D. Velegol and T. E. Mallouk, *Journal of the American Chemical Society*, 2013, **135**, 10557–10565.
49 S. Ketzetzi, J. de Graaf and D. J. Kraft, *arXiv preprint arXiv:2006.06384*, 2020.
50 O. Raz and A. Leshansky, *Physical Review E*, 2008, **77**, 055305.
51 D. Jeffrey and Y. Onishi, *The Quarterly Journal of Mechanics and Applied Mathematics*, 1981, **34**, 129–137.
52 H. Ohshima, *Colloid and Polymer Science*, 1999, **277**, 563–569.
53 L. Ren, D. Zhou, Z. Mao, P. Xu, T. J. Huang and T. E. Mallouk, *ACS nano*, 2017, **11**, 10591–10598.
54 G. M. Dougherty, K. A. Rose, J. B.-H. Tok, S. S. Pannu, F. Y. Chuang, M. Y. Sha, G. Chakarova and S. G. Penn, *Electrophoresis*, 2008, **29**, 1131–1139.
55 S. Ketzetzi, J. de Graaf, R. P. Doherty and D. J. Kraft, *Physical Review Letters*, 2020, **124**, 048002.
56 J. Riseman and J. G. Kirkwood, *The Journal of Chemical Physics*, 1950, **18**, 512–516.
57 B. Carrasco and J. Garcıa de la Torre, *The Journal of chemical physics*, 1999, **111**,

4817–4826.
58 F. Kümmel, B. ten Hagen, R. Wittkowski, I. Buttinoni, R. Eichhorn, G. Volpe, H. Löwen and C. Bechinger, *Physical review letters*, 2013, **110**, 198302.
59 B. Ten Hagen, F. Kümmel, R. Wittkowski, D. Takagi, H. Löwen and C. Bechinger, *Nature communications*, 2014, **5**, 4829.
60 B. Ten Hagen, R. Wittkowski, D. Takagi, F. Kümmel, C. Bechinger and H. Löwen, *Journal of Physics: Condensed Matter*, 2015, **27**, 194110.